MITSUBISHI ELECTRIC RESEARCH LABORATORIES
http://www.merl.com

Performance Analysis of Joint Opportunistic Scheduling and Receiver Design for MIMO-SDMA Downlink Systems

Pun, M-O; Kolvunen,V.; Poor, H.V.

TR2011-006 January 2011

Abstract

In this work, the sum-rate performance of joint opportunistic scheduling and receiver design (JOSRD) is analyzed for multiuser multiple-input-multiple output (MIMO) space-division multiple access (SDMA) downlink systems. In particular, we study linear rake receivers with selective combining, maximum ratio combining and optimal combining in which signals received from all antennas of each mobile terminal (MT) are linearly combined to improve the effective signal-to-interference-plus-noise ratios (SINRs). By exploiting limited feedback on the effective SINRs, the base station (BS) schedules simultaneous data transmission on multiple beams to the MTs with the largest effective SINRs. Using extreme value theory, the average sum-rates and their scaling laws for JOSRD are derived. In particular, it is shown that the limiting distribution of the effective signal-to-interference (SIR) is of the Frechet-type whereas that of the effective SINR converges to the Gumbel-type. Furthermore, the SIR-based sum-rate scaling laws are found to follow epsilon log K with 0 less-than epsilon less-than 1, which stands in contrast to the SINR-based scaling laws governed by the conventional log log K form. Both analytical and simulation results confirm that significant performance improvement can be achieved by incorporating low-complexity linear combining techniques into the design of scheduling schemes in MIMO-SDMA downlink systems.

IEEE Transactions on Communications

Performance Analysis of Joint Opportunistic Scheduling and Receiver Design for MIMO-SDMA Downlink Systems

Man-On Pun *Member, IEEE,* Visa Koivunen *Senior Member, IEEE,* and H. Vincent Poor *Fellow, IEEE*

***Abstract*—In this work, the sum-rate performance of joint opportunistic scheduling and receiver design (JOSRD) is analyzed for multiuser multiple-input-multiple output (MIMO) space-division multiple access (SDMA) downlink systems. In particular, we study linear rake receivers with selective combining, maximum ratio combining and optimal combining in which signals received from all antennas of each mobile terminal (MT) are linearly combined to improve the *effective* signal-to-interference-plus-noise ratios (SINRs). By exploiting limited feedback on the effective SINRs, the base station (BS) schedules simultaneous data transmission on multiple beams to the MTs with the largest effective SINRs. Using extreme value theory, the average sum-rates and their scaling laws for JOSRD are derived. In particular, it is shown that the limiting distribution of the effective signal-to-interference (SIR) is of the Frechet-type whereas that of the effective SINR converges to the Gumbel-type. Furthermore, the SIR-based sum-rate scaling laws are found to follow $\epsilon \log K$ with $0 < \epsilon < 1$, which stands in contrast to the SINR-based scaling laws governed by the conventional $\log \log K$ form. Both analytical and simulation results confirm that significant performance improvement can be achieved by incorporating low-complexity linear combining techniques into the design of scheduling schemes in MIMO-SDMA downlink systems.**

I. Introduction

Multiple-input multiple-output (MIMO) technology employing multiple transmit and receive antennas has emerged as one of the most promising techniques for broadband data transmissions in wireless communication systems [1]. In particular, recent studies have shown that MIMO can substantially increase the sum-rate capacity of a downlink system where a base station (BS) communicates simultaneously with multiple mobile terminals (MTs) [2]. However, the capacity achieving strategy using dirty paper coding (DPC) not only incurs high computational complexity but also requires perfect channel state information (CSI) available to the BS [2]. To circumvent these obstacles, opportunistic random beamforming with proportional fair scheduling (ORB-PFS) has been proposed in [3] as an effective means of achieving the asymptotic sum-rate capacity by exploiting multiuser diversity with limited channel feedback. In ORB-PFS, the downlink transmission time is divided in slots comprised of mini-slots. Users' channels are assumed to be approximately invariant during one slot but may vary from one slot to another. In the beginning of each slot, the BS broadcasts one pilot symbol weighted by a randomly generated complex vector (also referred to as the random beam). Then, each MT evaluates the signal-to-noise ratio (SNR) by exploiting the pilot signal and feeds the SNR information back to the BS. Taking into account fairness, the BS schedules data transmission to the MT with the best normalized instantaneous channel condition (with respect to its long-term channel condition) throughout the rest of the slot. In [3], it has been shown that ORB-PFS can achieve the sum-rate capacity fairly and asymptotically as the number of MTs increases. Recently, some extensions of [3] employing *multiple* beams have been developed [4], [5]. Regardless of the number of beams employed in [3]–[5], these opportunistic schemes schedule only one MT in each slot, and so can generally be considered to be the time-sharing scheduling schemes (TS-SS). In contrast, [6] has proposed a space-division multiple access-based opportunistic scheduling scheme (SDMA-SS) employing multiple orthonormal beams to serve multiple MTs *simultaneously* in each slot. Denote by M and N the number of transmit and receive antennas, respectively. It has been shown recently that the sum-rate of SDMA-SS and DPC grows linearly with M whereas that of TS-SS increases only linearly with $\min(M, N)$ [7]. Since we typically have $M \geq N$ in downlink, SDMA is more advantageous than TS-SS in terms of throughput. In addition to the more rapidly growing sum-rate scaling law, SDMA-SS is particularly attractive for practical systems with stringent latency requirements since multiple users can be served during each time slot.

In SDMA-SS, the BS broadcasts pilot signals weighted by multiple orthonormal beams in the beginning of each time slot [6]. For each single-antenna MT, it evaluates the signal-to-interference-plus-noise ratio (SINR) on each beam and feeds back information on its desired beam with the highest SINR. Assuming that each beam is requested by at least one MT, the BS awards each beam to the MT with the highest corresponding SINR among all MTs. For MTs with multiple

Manuscript received March 28, 2009; revised January 11, 2010; accepted September 17, 2010. The associate editor coordinating the review of this paper and approving it for publication was Nihar Jindal. This research was supported in part by the Croucher Foundation under a post-doctoral fellowship, and in part by the U. S. National Science Foundation under Grants ANI-03-38807 and CNS-06-25637. This work was presented in part at the IEEE International Conference on Communications 2008 (ICC'08), Beijing, China, May 2008.

Man-On Pun is with the Mitsubishi Electric Research Laboratories (MERL), Cambridge, MA 02139, USA. This work was done when he was a Croucher post-doctoral research fellow at Princeton University, Princeton, NJ (e-mail: mopun@ieee.org).

V. Koivunen is with the Signal Processing Laboratory, Helsinki University of Technology (HUT), Finland (e-mail: visa@wooster.hut.fi).

H. Vincent Poor is with the Department of Electrical Engineering, Princeton University, Princeton, NJ 08544 (e-mail: poor@princeton.edu).

Digital Object Identifier xxxx

receive antennas, [6] proposes to let each antenna compete for its desired beam as if it were an individual MT. As a result, each beam is assigned to a specific receive antenna of a chosen MT. It will be shown later that this scheme can be considered as a suboptimal form of the feedback scheme considered in this work with selection combining. Since signals received from the undesignated antennas of a chosen MT are discarded, [6] entails inefficient utilization of multiple receive antennas. Some extensions of [6] have been proposed to optimize the training and feedback design for SDMA systems with single-antenna MTs in [8], [9].

In this work, we consider an opportunistic MIMO-SDMA downlink system in which the BS as well as the MTs are equipped with multiple antennas. In contrast with [6], signals received from all antennas of a chosen MT are jointly exploited by the feedback schemes considered in this work to improve the effective SINR through the use of low-complexity linear combining techniques. Then, information about $Q \leq M$ beams of highest effective SINRs is returned to the BS and employed as the scheduling metric. Using extreme value theory, we propose a systematic approach to quantify the average sum-rates and scaling laws. More specifically, we first prove that the limiting distribution of the effective signal-to-interference ratio (SIR) obtained with different linear combining techniques is of the Frechet-type whereas that of the effective SINR is of the Gumbel-type. Then, we derive the average sum-rates and scaling laws for opportunistic scheduling schemes with different combining techniques by exploiting their corresponding limiting distributions of the effective SIR and SINR, respectively. It is found that the SIR-based scaling laws follow $\epsilon \log K$ with $0 < \epsilon < 1$ whereas the SINR-based scaling laws obey the $\log \log K$ form, where K is the number of MTs. Furthermore, comparison of the SIR and SINR-based analyses suggests that, for interference-limited applications such as SDMA-based systems, the SIR-based analysis has reduced computational complexity and is more effective in capturing the asymptotic system performance of the scheduling schemes under consideration with higher fidelity. Both analytical and simulation results confirm that incorporating low-complexity linear combining techniques into the design of opportunistic scheduling and beamforming schemes can provide substantial throughput advantages for MIMO-SDMA downlink systems.

Before proceeding further, the main contributions distinguishing this work from other existing works should be emphasized. The notion of joint opportunistic scheduling and receiver design (JOSRD) was first pioneered in [10]. However, [10] only considers zero-forcing (ZF) receivers whose performance was evaluated via simulation. In contrast, this work concentrates on establishing a theoretical framework to analyze the sum-rate performance provided by joint opportunistic scheduling and receiver design using different types of receivers. Furthermore, unlike [11]–[13] in which single-antenna receivers are considered, this work analytically exemplifies the significance of receiver design via more effective utilization of multiple receive antennas. Finally, despite the fact that [14]–[17] also consider receivers equipped with multiple antennas, the feedback scheme considered in their works is rather different from that in this work. Indeed, the feedback scheme studied in [14]–[17] and this work stand for two very different approaches in interference mitigation for MIMO-SDMA: the feedback scheme in [14]–[17] is designed to eliminate interference by the BS via ZF beamforming whereas interference is mitigated by the receivers in our work. More specifically, [14]–[17] capitalize on their feedback comprised of quantized channel direction information (CDI) and channel quality information (CQI). Thanks to the quantized CDI, ZF beamforming can be employed at the BS to ensure that all arriving beams remain orthogonal at each MT. As a result, inter-beam interference can be completely eliminated in the absence of CDI quantization errors in [14]–[17]. In contrast, CDI is *not* employed in our feedback scheme for the sake of simple and low-complexity feedback design. As a result, the lack of CDI in our feedback scheme prevents the BS from performing ZF beamforming in this work. Thus, the detrimental impact caused by inter-beam interference is non-negligible and has to be accurately characterized in analysis. Both analytical and simulation results have confirmed that effective interference mitigation plays an important role in improving system performance for the feedback scheme considered in this work.

The rest of the paper is organized as follows. We introduce the signal model for MIMO-SDMA downlink transmissions in Sec. II. Then, opportunistic scheduling and beamforming schemes are reviewed for MIMO-SDMA downlink systems with linear combining in Sec. III. SIR and SINR-based theoretical analyses on the average sum-rates and scaling laws for JOSRD are derived in Secs. IV and V, respectively. Comparisons between the SIR and SINR-based theoretical analyses are elaborated in Sec. VI. Finally, simulation results are shown in Sec. VII while the conclusion is given in Sec. VIII.

Notation: Vectors and matrices are denoted by boldface letters. $\|\cdot\|$ represents the Euclidean norm of the enclosed vector and $|\cdot|$ denotes the amplitude of the enclosed complex-valued quantity. $\boldsymbol{I}_N$ is the $N \times N$ identity matrix. $[\boldsymbol{A}]_{i,j}$ and $[\boldsymbol{a}]_i$ indicate the element at the i-th row and j-th column of matrix $\boldsymbol{A}$ and the i-th entry of vector $\boldsymbol{a}$, respectively. We use $E\{\cdot\}$, $(\cdot)^*$, $(\cdot)^T$ and $(\cdot)^H$ for expectation, complex conjugation, transposition and Hermitian transposition. Finally, $\log$ and $\ln$ are the logarithms to the base 2 and e, respectively.

II. Signal Model

We consider the opportunistic MIMO-SDMA downlink system depicted in Fig. 1 where the BS is equipped with M transmit antennas and each of the K MTs has N receive antennas with $N \leq M$. Let $\{\boldsymbol{a}_m; m = 1, 2, \cdots, M\}$ be a vector set containing M orthornormal beamforming vectors of length M. We focus on a particular time slot during which a beamforming vector set $\{\boldsymbol{a}_m\}$ has been chosen from a common codebook shared by the BS and MTs. During the p-th mini-slot, the transmitted signal can be expressed as

$$\boldsymbol{x}(p) = \sum_{m=1}^{M} \boldsymbol{a}_m s_m(p) = \boldsymbol{A}\boldsymbol{s}(p), \tag{1}$$

where $\boldsymbol{A} = [\boldsymbol{a}_1, \boldsymbol{a}_2, \cdots, \boldsymbol{a}_M]$ is the unitary beamforming matrix with $\boldsymbol{A}^H\boldsymbol{A} = \boldsymbol{I}_M$ and $\boldsymbol{s}(p) = [s_1(p), s_2(p), \cdots, s_M(p)]^T$

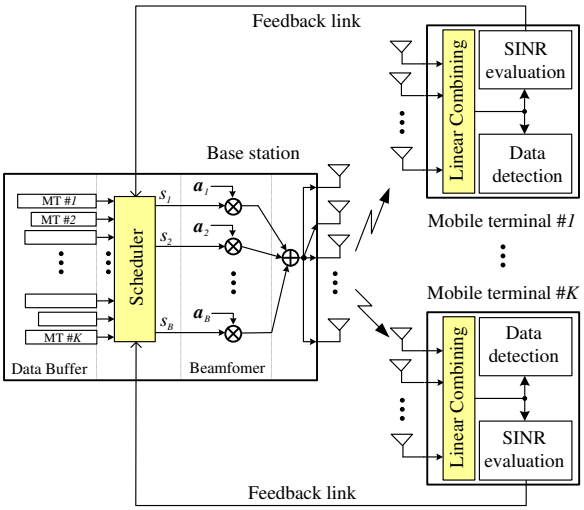

Fig. 1. A block diagram of the opportunistic MIMO SDMA downlink system under consideration.

with $E\left\{|s_m(p)|^2\right\} = 1$ is the data vector transmitted in the p-th mini-slot. Thus, the total average transmission power is set to M [6].

For notational simplicity, we drop the temporal index p in the sequel. Assuming that each MT experiences independent and identically-distributed (i.i.d.) frequency-flat Rayleigh fading, we use $\boldsymbol{h}_{k,j}$ to denote the $1 \times M$ channel gain vector with the m-th entry, $[\boldsymbol{h}_{k,j}]_m$, representing the channel gain from the m-th transmit antenna of the BS to the j-th receive antenna of the k-th MT. Thus, the signal received by the j-th receive antenna of the k-th MT can be expressed as:

$$r_{k,j} = \sqrt{P_k}\boldsymbol{h}_{k,j}\boldsymbol{x} + n_{k,j}, \quad 1 \le j \le N \tag{2}$$

where P_k is the average input SNR for the kth MT and $n_{k,j}$ is a complex, circular additive Gaussian noise that is assumed to be spatially and spectrally white. Without loss of generality, all signal powers are normalized with respect to the noise power. As a result, the entries of $\boldsymbol{h}_{k,j}$ and $n_{k,j}$ are modeled as $\mathcal{CN}(0,1)$.

By stacking the signals received by N antennas into a column vector, we can rewrite (2) into the following matrix form.

$$\boldsymbol{r}_k = \sqrt{P_k}\boldsymbol{H}_k\boldsymbol{x} + \boldsymbol{n}_k, \tag{3}$$

where $\boldsymbol{r}_k = [r_{k,1}, r_{k,2}, \cdots, r_{k,N}]^T$, $\boldsymbol{n}_k = [n_{k,1}, n_{k,2}, \cdots, n_{k,N}]^T$ and $\boldsymbol{H}_k$ is the k-th MT's channel matrix defined as $\boldsymbol{H}_k = \left[\boldsymbol{h}_{k,1}^T, \boldsymbol{h}_{k,2}^T, \cdots, \boldsymbol{h}_{k,N}^T\right]^T$. Similar to [5], [6], we assume that each MT has obtained perfect knowledge of its own channel matrix $\boldsymbol{H}_k$ by means such as training. Furthermore, it is important to observe that the channel matrix in (3) is fat. As a result, the MTs in the MIMO-SDMA systems have only N degrees of freedom to suppress maximum $M-1$ interfering beams. Without effective interference suppression, the system performance will be degraded poorly due to the lack of degrees of freedom for interference suppression.

Thus, the SINR of the m-th beam observed by the j-th receive antenna of the k-th MT is given by

$$\gamma_{k,j,m}^{(\text{Observed})} = \frac{|\boldsymbol{h}_{k,j}\boldsymbol{a}_m|^2}{\sum\limits_{\substack{i=1 \\ i\neq m}}^{M} |\boldsymbol{h}_{k,j}\boldsymbol{a}_i|^2 + \dfrac{1}{P_k}}, \tag{4}$$

for $k = 1, 2, \cdots, K$, $j = 1, 2, \cdots, N$ and $m = 1, 2, \cdots, M$. In the sequel, $\gamma_{k,j,m}^{(\text{Observed})}$ is referred to as the *observed* SINR whereas the *effective* SINR stands for the SINR obtained by linearly combining signals from all received antennas. It will become evident in the following analysis that $\gamma_{k,j,m}^{(\text{Observed})}$ is less than the effective SINR. As a result, the conventional scheduling schemes based on $\gamma_{k,j,m}^{(\text{Observed})}$ such as [6] are suboptimal in terms of system throughput, compared to the the effective SINR-based schemes considered in this work.

III. Joint opportunistic scheduling and receive design (JOSRD)

A. Scheme description

Recall that [10] considers an opportunistic scheduling scheme in conjunction with ZF receivers. In this section, we generalize this concept to explore opportunistic scheduling with different linear receiver structures. More specifically, we design beamforming and scheduling schemes for MIMO-SDMA by exploiting the effective SINR obtained with different linear combining techniques.

In the beginning of each time slot, each MT evaluates the effective SINR for each beam and feeds information about M effective SINRs back to the BS. More specifically, the effective SINRs of the m-th beam at the k-th MT obtained with selection combining (SC), maximum ratio combining (MRC) and optimum combining (OC) techniques can be computed as follows [18]:

$$\gamma_{k,m}^{(\text{SC})} = \max_{1\le n\le N}\left\{\frac{|\boldsymbol{h}_{k,n}\boldsymbol{a}_m|^2}{\sum\limits_{i\neq m}|\boldsymbol{h}_{k,n}\boldsymbol{a}_i|^2 + 1/P_k}\right\} \tag{5}$$

$$\gamma_{k,m}^{(\text{MRC})} = \frac{\|\boldsymbol{H}_k\boldsymbol{a}_m\|^4}{\sum\limits_{i\neq m}\left|\boldsymbol{a}_m^H\boldsymbol{H}_k^H\boldsymbol{H}_k\boldsymbol{a}_i\right|^2 + \|\boldsymbol{H}_k\boldsymbol{a}_m\|^2/P_k}, \tag{6}$$

$$\gamma_{k,m}^{(\text{OC})} = \boldsymbol{a}_m^H\boldsymbol{H}_k^H\left[\boldsymbol{H}_k\sum_{i\neq m}\boldsymbol{a}_i\boldsymbol{a}_i^H\boldsymbol{H}_k^H + \frac{\boldsymbol{I}_N}{P_k}\right]^{-1}\boldsymbol{H}_k\boldsymbol{a}_m. \tag{7}$$

Note that (7) performs active interference suppression by exploiting the interference structure whereas (5) and (6) simply intend to amplify the desired signal. It will be shown later that this characteristic interference-suppression feature of OC enables the scheduling scheme with OC to considerably outperform those with SC and MRC.

Upon receiving the effective SINR information from all MTs, the BS schedules and starts data transmission to multiple MTs with the largest effective SINRs on different beams until

the end of the current time slot. At each chosen MT, received signals from all antennas are linearly combined using one of the above linear combining techniques, followed by data detection. It is worth noting that the probability of awarding multiple beams to the same MT is rather small, as the number of MTs grows large. Furthermore, recall that the minimum mean squared error (MMSE) and zero-forcing (ZF) receiver structures for MIMO receivers amount to combiners using OC and MRC for each beam, respectively [18]. As a result, an MT assigned with multiple beams can focus on one assigned beam at a time using the chosen combining technique while regarding all other beams as interfering sources.

B. Fairness in scheduling

Unlike the TS-SS that requires PFS to maintain fair scheduling among all MTs, the SDMA-based scheduling schemes have been shown to guarantee fairness in scheduling even in a near-far environment [6]. Intuitively speaking, since the SDMA-based systems are interference-limited, an MT with a larger P_k will receive stronger desired signals as well as interference. Consequently, the effective SINR of each beam perceived by an MT is mainly determined by the *alignment* of the MT's instantaneous channel vectors and the beam under consideration.

C. Reduced-feedback JOSRD (RF-JOSRD)

Further feedback reduction for JOSRD can be achieved by resorting to some ad-hoc feedback approaches. For instance, rather than returning M SINRs to the BS, each MT can only feed back information about its largest $Q < M$ SINRs to the BS. This approach is similar to that adopted in [6] where $Q = N$. In the sequel, this alternative feedback scheme is referred to as the reduced-feedback JOSRD (RF-JOSRD). We will concentrate our following analysis on JOSRD in which each MT returns *all* M SINRs to the BS while evaluating the performance of RF-JOSRD via simulation in Sec. VII.

In the next two sections, SIR and SINR-based theoretical analyses on the average sum-rates and scaling laws of the joint opportunistic scheduling and receiver design scheme are derived using extreme value theory [19]. In contrast with the analytical approach adopted in [6] where upper and lower bounds are employed to approximate the scaling laws, a systematic approach is developed to derive the average sum-rates and scaling laws. Most specifically, for a given SIR/SINR parent distribution function, the proposed approach first determines the domain of attraction of its limiting distribution before computing the corresponding normalizing factors. From the resulting limiting distribution, the average sum-rates and scaling laws can be routinely derived. To shed light on system performance in the following theoretical analysis, we concentrate on a homogenous network in this work, assuming all MTs have the same average SNR, i.e. $P_k = P_s$ for $k = 1, 2, \cdots, K$. While this homogenous assumption is commonly made in the literature [6], [12], [17], theoretical analysis on the performance of opportunistic scheduling in heterogeneous networks remains a challenging open question. This is partially because that the design objective in heterogeneous networks becomes twofold: maximizing system throughput while maintaining fairness among heterogeneous users. As a result, the analysis becomes rather complicated due to the necessity of characterizing both fairness and weighted sum-rate performance in the presence of different average SNRs.

IV. SIR-based Throughput Analysis

In this section, we first consider the interference-limited scenario where the interference power is much larger than the additive noise power, which is the typical scenario for SDMA-based systems. As a result, the SINRs given in (5)-(7) can be well approximated by their corresponding SIRs given by:

$$\rho_{k,m}^{(\mathrm{SC})} = \max_{1\le n\le N}\left\{\frac{|\boldsymbol{h}_{k,n}\boldsymbol{a}_m|^2}{\sum_{i\neq m}|\boldsymbol{h}_{k,n}\boldsymbol{a}_i|^2}\right\}, \quad (8)$$

$$\rho_{k,m}^{(\mathrm{MRC})} = \frac{\|\boldsymbol{H}_k\boldsymbol{a}_m\|^4}{\sum_{i\neq m}\left|\boldsymbol{a}_m^H\boldsymbol{H}_k^H\boldsymbol{H}_k\boldsymbol{a}_i\right|^2}, \quad (9)$$

$$\rho_{k,m}^{(\mathrm{OC})} = \boldsymbol{a}_m^H\boldsymbol{H}_k^H\left[\boldsymbol{H}_k\sum_{i\neq m}\boldsymbol{a}_i\boldsymbol{a}_i^H\boldsymbol{H}_k^H\right]^{-1}\boldsymbol{H}_k\boldsymbol{a}_m, \quad (10)$$

where a necessary condition required to guarantee the invertibility of $\boldsymbol{H}_k\sum_{i\neq m}\boldsymbol{a}_i\boldsymbol{a}_i^H\boldsymbol{H}_k^H$ in (10) is $M > N$.

Assuming $\rho_{k,m}$ for $k = 1, 2, \cdots, K$, are i.i.d. with a cumulative distribution function (CDF) $F_X(x)$, the CDF of the maximum, $\rho_m^* = \max_k \rho_{k,m}$, is given by $[F_X(x)]^K$. Hence, the resulting average sum-rate of JOSRD can be computed as [2]

$$C = E\left\{\sum_{m=1}^{M}\log\left(1+\max_k\rho_{k,m}\right)\right\}, \quad (11)$$

$$= M\int_0^\infty \log(1+x)\, d\left[F_X(x)\right]^K. \quad (12)$$

In the following, we first find the $F_X(x)$ functions obtained with different combining techniques before establishing their corresponding limiting distributions.

A. Statistics of effective SIR

The CDF of the effective SIRs obtained with different combining techniques can be shown as follows [6], [20].

$$F_X^{(\mathrm{Observed})}(x) = 1 - \frac{1}{(1+x)^{M-1}}, \quad (13)$$

$$F_X^{(\mathrm{SC})}(x) = \left[1 - \frac{1}{(1+x)^{M-1}}\right]^N, \quad (14)$$

$$F_X^{(\mathrm{MRC})}(x) = 1 - \frac{1}{(1+x)^{M-1}} - \sum_{p=1}^{N-1} \binom{M+N-p-2}{M-2} \frac{x^{N-p}}{(1+x)^{M+N-p-1}}, \quad (15)$$

$$F_X^{(\mathrm{OC})}(x) = 1 - \frac{1}{(1+x)^{M-N}} - \sum_{p=1}^{N-1} \binom{M-p-1}{M-N-1} \frac{x^{N-p}}{(1+x)^{M-p}}. \quad (16)$$

We can easily verify that (14) is identical to (15) for $M = N = 2$, which implies that SC and MRC have the same performance at high SNR for $M = N = 2$.

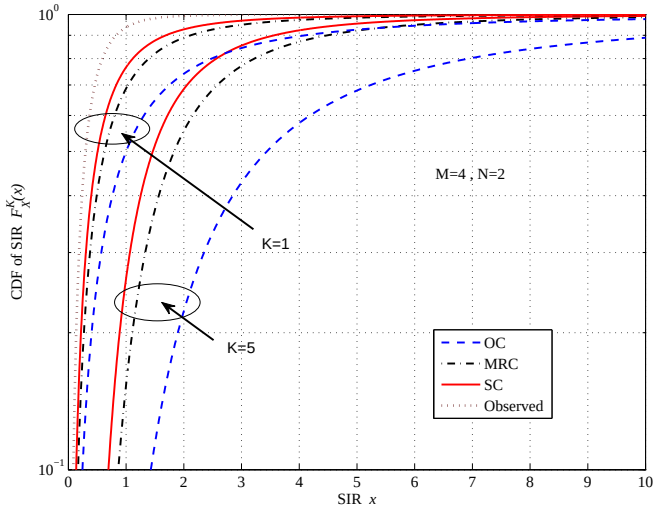

Fig. 2. CDF's of SIR obtained with K MTs for different combining techniques with $M = 4$ and $N = 2$.

From (14)-(16), the CDF of $\max_k \rho_{k,m}$ obtained with different combining techniques, $[F_X(x)]^K$, can be computed correspondingly. Figure 2 shows the CDFs of the observed SIR and the maximum effective SIR, $[F_X(x)]^K$, derived from (13)-(16) for the case of $M = 4$, $N = 2$ and $K = 1, 5$. The selection of $M = 4$ and $N = 2$ is due to the considerable practical interests in systems with those parameters. Figure 2 indicates that the CDF of the effective SIR obtained with OC has a heavier tail than those obtained with MRC and SC. As a result, it is more probable for OC to achieve a larger effective SIR than the others for given M and N, which leads to a higher system throughput. Furthermore, it is evident from Fig. 2 that the tail behavior of OC improves more significantly over MRC and SC as the number of MTs, K, increases.

It is interesting to compare JOSRD using SC and that proposed in [6]. In [6], a receive antenna at each MT is regarded as an individual MT. Under some mild assumptions, it has been shown in [6] that the maximum SINR over all beams observed by a particular receive antenna is equal to the maximum SINR for that best beam observed by all N receive antennas. As a result, the CDF of the maximum effective SIR for the m-th beam at the k-th MT in the interference-limited environment can be approximated by

$$\left[F_X^{(\mathrm{SH})}(x)\right]^{K_m} \approx \left[1 - \frac{1}{(1+x)^{M-1}}\right]^{NK_m}, \quad (17)$$

where $K_m \leq K$ is the number of requests for the m-th beam from the K MTs with $\sum_{m=1}^{M} K_m = KN$. Comparison between (17) and $\left[F_X^{(\mathrm{SC})}(x)\right]^K = \left[1 - \frac{1}{(1+x)^{M-1}}\right]^{NK}$, reveals that [6] can be considered as a suboptimal form of JORD with selection combining. The suboptimality is caused by the fact that JOSRD with SC requires information on all M beams from each MT whereas [6] simply feeds back information on N selected beams. Thus, [6] can be regarded as a special case of JOSRD using SC but with further reduced feedback as discussed in Sec. III-C. However, as will be shown shortly, even the performance of the full-feedback scheduling scheme with SC is rather unimpressive compared to schemes employing other combining techniques.

B. Asymptotic throughput

In order to investigate the performance of JOSRD while keeping the analytical complexity tractable, we concentrate the following analysis on a system of high practical interest, i.e. $M = 4$ and $N = 2$. The results can be extended to other values of M and N in a straightforward fashion. Due to space limitations, we will only detail the derivation for the case of OC and provide the final results for JOSRD with the other two combining techniques.

We first investigate the asymptotic behavior of $F_{X_{(K)}}(x) = [F_X(x)]^K$ as K increases. For $M = 4$ and $N = 2$, (16) becomes

$$F_X^{(\mathrm{OC})}(x) = 1 - \frac{1+3x}{(1+x)^3}. \quad (18)$$

It is known in the context of extreme value theory that the limiting distribution of $F_{X_{(K)}}(x) = [F_X(x)]^K$, if it exists, belongs to one of three domains of attraction [19]. Fortunately, we can easily prove that the parent distribution given in (18) is of the Pareto type and satisfies the following equation

$$\lim_{x\to\infty} \frac{1 - F_X^{(\mathrm{OC})}(x)}{1 - F_X^{(\mathrm{OC})}(cx)} = c^2, \quad c > 0 \quad (19)$$

which is a necessary and sufficient condition for the resulting limiting distribution being of the Frechet type. Consequently, $F_{X_{(K)}}(x) = [F_X(x)]^K$ converges to the following Frechet-type distribution.

$$F_{X_{(K)}}^{(\mathrm{OC})}(a_K^{(\mathrm{OC})} x) = \begin{cases} 0 & x \leq 0 \\ \exp\{-x^{-2}\} & x > 0 \end{cases}, \quad (20)$$

where the normalizing factor $a_K^{(\mathrm{OC})}$ can be computed from the so-called characteristic extreme of (18) as follows:

$$F_X^{(\mathrm{OC})}(a_K) = 1 - \frac{1}{K}, \quad (21)$$

$$a_K^{(\mathrm{OC})} \approx \sqrt{3K} - 1. \quad (22)$$

Thus, we have

$$P_{X_{(K)}}^{(\mathrm{OC})}\left(X_{(K)} \leq \left(\sqrt{3K}-1\right)x\right) \approx \exp\left\{-x^{-2}\right\}, \quad (23)$$

for $x \geq 0$, or equivalently,

$$P_{X_{(K)}}^{(\mathrm{OC})}\left(X_{(K)} \leq x\right) \approx \exp\left\{-\left(\sqrt{3K}-1\right)^2 x^{-2}\right\}. \quad (24)$$

Substituting (24) into (12), we have the average sum-rate obtained with OC as follows.

$$\begin{aligned} & C^{(\mathrm{OC})} \\ \approx\ & 4\int_0^\infty \log(1+x)\, d\left[\exp\left\{-\frac{\left(\sqrt{3K}-1\right)^2}{x^2}\right\}\right], \quad (25) \\ =\ & -4\int_0^\infty \log(1+x)\, d\left[1-\exp\left\{-\frac{\left(\sqrt{3K}-1\right)^2}{x^2}\right\}\right], \quad (26) \\ =\ & \frac{4}{\ln 2}\int_0^\infty \frac{1-\exp\left\{-\frac{\left(\sqrt{3K}-1\right)^2}{x^2}\right\}}{1+x}\, dx, \quad (27) \end{aligned}$$

where the last equality is obtained by using the integration by parts. Since the closed-form expression of (27) is non-trivial, we can evaluate the average sum-rate obtained with OC by resorting to numerical methods.

Similarly, we can derive the average sum-rates obtained with MRC and SC as follows.

$$C^{(\mathrm{MRC})} \approx \frac{4}{\ln 2}\int_0^\infty \frac{1-\exp\left\{-\frac{\left(\sqrt[3]{4K}-1\right)^3}{x^3}\right\}}{1+x}\, dx, \quad (28)$$

$$C^{(\mathrm{SC})} \approx \frac{4}{\ln 2}\int_0^\infty \frac{1-\exp\left\{-\frac{\left(\sqrt[3]{2K}-1\right)^3}{x^3}\right\}}{1+x}\, dx. \quad (29)$$

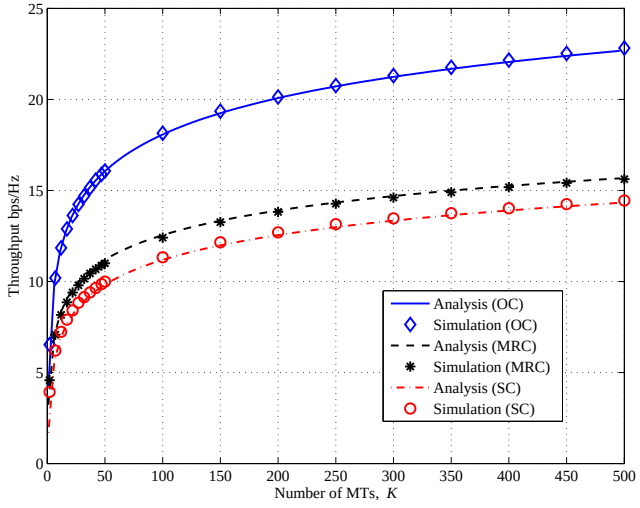

Fig. 3. Comparison of analytical and simulated average sum-rates as a function of the number of MTs with $M = 4$, $N = 2$ and $\sigma_k^2 = 0$.

Figure 3 compares the analytical average sum-rates shown in (27)-(29) with the simulation results obtained in a *noise-free* scenario. It is evident from Fig. 3 that the analytical and simulated results are in accord with each other. In particular, despite that the average sum-rates obtained in (27)-(29) have been derived based on the assumption of a large K, Fig. 3 suggests that (27)-(29) are quite accurate even for smaller K values. Furthermore, inspection of Fig. 3 reveals that the average sum-rate obtained with OC is more than 40% larger than those obtained with SC and MRC for $M = 4$ and $N = 2$ in the noise-free scenario, which is attributed to the inherent interference suppression feature of OC.

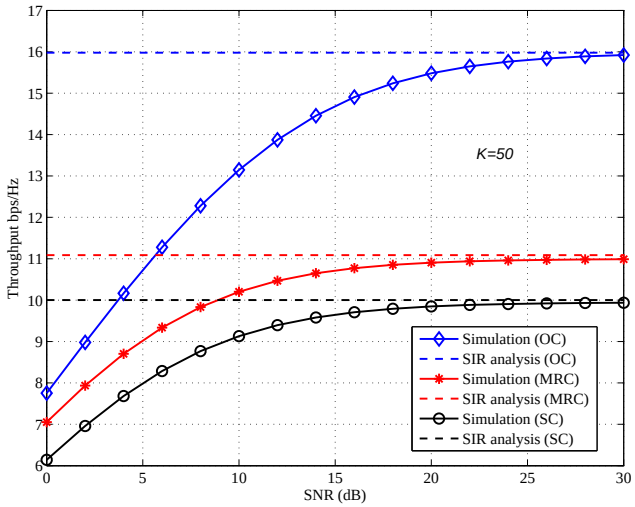

Fig. 4. Real system simulation versus SIR-based analytical results with $M = 4$, $N = 2$ and $K = 50$.

Furthermore, Figure 4 compares the SIR-based analytical sum-rates with the simulation results derived from real systems with $M = 4$, $N = 2$ and $K = 50$ over SNR of $[0, 30]$ dB. Figure 4 shows that the simulation results approach the SIR-based analytical results as SNR increases. In particular, the discrepancy between the SIR-based analytical and simulation results is reduced to less than 10% for SNR larger than 15 dB, which is within the operating SNR range for practical systems.

C. Scaling law

To provide insights into the influence of the number of MTs, K, on the system throughput, we investigate the scaling laws of JOSRD as a function of K, assuming K is sufficiently large. Similar to the previous section, we concentrate on the scaling law for JOSRD with OC whereas only the final results for those with MRC and SC are provided. To derive the scaling law of the scheme with OC, we first rewrite (27) by letting $v = \frac{1}{x}$, where $v \in (0^+, \infty)$. Thus, (27) becomes

$$\begin{aligned} & C^{(\mathrm{OC})} \\ \approx\ & \frac{4}{\ln 2}\int_{0^+}^\infty \frac{1-\exp\left\{-\left(\sqrt{3K}-1\right)^2 v^2\right\}}{(1+v)\, v}\, dv, \quad (30) \end{aligned}$$

$$\approx \frac{4}{\ln 2}\int_{0+}^{\frac{2}{\sqrt{3K}-1}} \frac{1-\exp\left\{-\left(\sqrt{3K}-1\right)^2 v^2\right\}}{(1+v)\,v}\,dv + \frac{4}{\ln 2}\int_{\frac{2}{\sqrt{3K}-1}}^{\infty} \frac{1}{(1+v)\,v}\,dv, \quad (31)$$

where the last approximation is obtained by exploiting the fact that $1-e^{-\xi}\approx 1$, for $\xi \geq 4$.

Taking the limit of (31) as K tends to infinity, it is easy to show that the limit of the second term on the right hand side (R.H.S.) takes the following form

$$\lim_{K\to\infty} \frac{\frac{4}{\ln 2}\int_{\frac{2}{\sqrt{3K}-1}}^{\infty} \frac{1}{(1+v)v}\,dv}{4\log\left(\sqrt{3K}\right)} = 1, \quad (32)$$

whereas the limit of the first term becomes negligibly small as $\lim_{K\to\infty} \frac{2}{\sqrt{3K}-1} = 0$. As a result, the scaling law for JOSRD with OC is given by

$$\lim_{K\to\infty} \frac{C^{(\mathrm{OC})}}{4\log\left(\sqrt{3K}\right)} = 1. \quad (33)$$

Similarly, we can obtain the scaling laws for the schemes with MRC and SC as follows.

$$\lim_{K\to\infty} \frac{C^{(\mathrm{MRC})}}{4\log\left(\sqrt[3]{4K}\right)} = 1 \quad (34)$$

$$\lim_{K\to\infty} \frac{C^{(\mathrm{SC})}}{4\log\left(\sqrt[3]{2K}\right)} = 1 \quad (35)$$

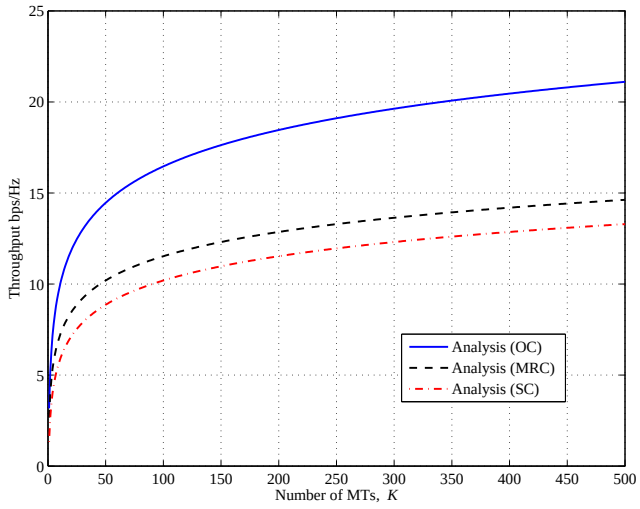

Fig. 5. Scaling laws as a function of the number of MTs with $M=4$ and $N=2$.

Figure 5 depicts the scaling laws obtained in (33), (34) and (35). Comparison between Figs. 3 and 5 indicates that the scaling laws approximately follow the simulation results.

It is rather surprising to observe that the analytical results established in this section are different from those reported in the literature [3], [6] in two aspects. First, the limiting distribution of the effective SIR is of the Frechet type, rather than the Gumbel type. Second, the SIR-based scaling laws derived in (33), (34) and (35) follow the form of $\epsilon \log K$ with $0<\epsilon<1$, which stands in contrast to the conventional $\log\log K$ form. In the following, we first repeat our analysis above by replacing the effective SIR with the effective SINR followed by some remarks on the comparisons between the SIR and SINR-based analyses.

V. SINR-BASED THROUGHPUT ANALYSIS

Assuming $\gamma_{k,m}$ in (5)-(7) are i.i.d. for $k=1,2,\cdots,K$ with CDF $F_Y(y)$, the SINR-based average sum-rate is given by

$$R = M\int_0^{\infty} \log(1+y)\; d\left[F_Y(y)\right]^K. \quad (36)$$

Following the approach established in the previous section, we will derive the parent distribution $F_Y(y)$ obtained with different linear combining techniques and subsequently, their corresponding limiting distributions, i.e. $\lim_{K\to\infty}[F_Y(y)]^K$. By exploiting the limiting distributions, we derive the average sum-rates and the corresponding scaling laws.

A. Statistics of effective SINR

The CDFs of the effective SINR obtained with SC and OC are given in the following forms, respectively [6], [21].

$$F_Y^{(\mathrm{SC})}(y) = \left[1-\frac{\exp\{-y/P_s\}}{(1+y)^{M-1}}\right]^N, \quad (37)$$

$$F_Y^{(\mathrm{OC})}(y) = 1-\exp\left\{-\frac{y}{P_s}\right\}\sum_{n=1}^{N}\frac{A_n(y)}{(n-1)!}\left(\frac{y}{P_s}\right)^{n-1}, \quad (38)$$

where

$$A_n(y) = \begin{cases} \dfrac{1+\sum_{i=1}^{N-n}\binom{M-1}{i}y^i}{(1+y)^{M-1}} & N < M-1+n, \\ 1 & \text{otherwise.} \end{cases} \quad (39)$$

Furthermore, the probability density function (PDF) of the effective SINR obtained with MRC has been shown as [20], [22]

$$f_Y^{(\mathrm{MRC})}(y) = \frac{y^{N-1}e^{-y/P_s}}{\Gamma(N)\Gamma(M-1)}\sum_{\ell=0}^{N}\binom{N}{\ell}\frac{1}{P_s^{N-\ell}}\frac{\Gamma(M-1+\ell)}{(1+y)^{M-1+\ell}}, \quad (40)$$

where $\Gamma(z)=(z-1)!$ is the standard Gamma function for any positive integer z.

Due to space limitations, only the details of the derivation for JOSRD with OC are provided in the following, whereas final results for MRC and SC are summarized at the end of this section. To compare the following SINR-based analysis with the previous SIR-based analysis, we also concentrate on the MIMO-SDMA system with $M=4$ and $N=2$.

B. Analysis for JOSRD with OC

The CDF and PDF of the effective SINR obtained with OC for $M = 4$ and $N = 2$ can be readily derived from (38) as

$$F_Y^{(\mathrm{OC})}(y) = 1 - \frac{\exp\{-y/P_s\}}{(1+y)^2} - \frac{2y\exp\{-y/P_s\}}{(1+y)^3} - \frac{y\exp\{-y/P_s\}}{P_s(1+y)^3}, \quad (41)$$

and

$$f_Y^{(\mathrm{OC})}(y) = \frac{y\exp\{-y/P_s\}}{P_s^2(1+y)^4}\left[(3P_s+1)y + \left(6P_s^2+6P_s+1\right)\right], \quad (42)$$

respectively.

It is easy to verify that

$$\lim_{x\to\infty}\frac{1-F_Y^{(\mathrm{OC})}(y)}{f_Y^{(\mathrm{OC})}(y)} = P_s > 0, \quad (43)$$

which is the necessary and sufficient condition for the limiting distribution of $\left[F_Y^{(\mathrm{OC})}(y)\right]^K$ being of the Gumbel type [19]. As a result, $F_{Y_{(K)}}^{(\mathrm{OC})}(y) = \left[F_Y^{(\mathrm{OC})}(y)\right]^K$ converges to the following Gumbel-type distribution [19].

$$F_{Y_{(K)}}^{(\mathrm{OC})}\left(a_K^{(\mathrm{OC})}y + b_K^{(\mathrm{OC})}\right) = \exp\{-\exp\{-y\}\}, \quad y \geq 0 \quad (44)$$

or equivalently,

$$F_{Y_{(K)}}^{(\mathrm{OC})}(y) = \exp\left\{-\exp\left\{-\frac{y}{a_K^{(\mathrm{OC})}} + \frac{b_K^{(\mathrm{OC})}}{a_K^{(\mathrm{OC})}}\right\}\right\}, \quad y \geq 0, \quad (45)$$

where $a_K^{(\mathrm{OC})}$ and $b_K^{(\mathrm{OC})}$ are normalizing factors affecting the shape and location of the limiting distribution, respectively. From extreme value theory, $b_K^{(\mathrm{OC})}$ and $a_K^{(\mathrm{OC})}$ can be computed from the characteristic extreme of (41) as [19]

$$1 - F_Y^{(\mathrm{OC})}\left(b_K^{(\mathrm{OC})}\right) = \frac{1}{K}, \quad (46)$$

$$a_K^{(\mathrm{OC})} = {F_Y^{(\mathrm{OC})}}^{-1}\left(1 - \frac{1}{Ke}\right) - b_K^{(\mathrm{OC})}. \quad (47)$$

Since (46) is an exponential-linear equation of $b_K^{(\mathrm{OC})}$, it is non-trivial to obtain the exact solution of $b_K^{(\mathrm{OC})}$ in a closed form. Fortunately, since $1 - F_{Y_{(K)}}^{(\mathrm{OC})}$ monotonically decreases from 1 to 0 whereas $1/K \in [1, 0)$ for $K = 1, 2, \cdots, \infty$, there always exists a unique solution to (46). Thus, we can resort to numerical methods to compute a solution of $b_K^{(\mathrm{OC})}$ which is referred to as the *numerical* solution in the sequel. Similarly, we can also show that there always exists a unique numerical solution of $a_K^{(\mathrm{OC})}$ that can be found by resorting to numerical methods.

Rather than the numerical solutions of $b_K^{(\mathrm{OC})}$ and $a_K^{(\mathrm{OC})}$, if we assume K is sufficiently large, we can exploit the following approximation

$$\frac{\exp\left\{-b_K^{(\mathrm{OC})}/P_s\right\}}{\left(1+b_K^{(\mathrm{OC})}\right)^2} \approx \frac{b_K^{(\mathrm{OC})}\exp\left\{-b_K^{(\mathrm{OC})}/P_s\right\}}{\left(1+b_K^{(\mathrm{OC})}\right)^3}. \quad (48)$$

As a result, $b_K^{(\mathrm{OC})}$ and $a_K^{(\mathrm{OC})}$ can be approximated by the following expressions.

$$b_K^{(\mathrm{OC})} \approx P_s\ln\left(\left(3+1/P_s\right)K\right) - 2P_s\ln\left(P_s\ln K\right), \quad (49)$$

$$a_K^{(\mathrm{OC})} \approx P_s. \quad (50)$$

Substituting (45) into (36) followed by some mathematical manipulations, we can show the average sum-rate obtained with OC is given by:

$$R^{(\mathrm{OC})} = \frac{4}{\ln 2}\int_0^\infty \frac{1-\exp\left\{-\exp\left\{-\frac{y}{a_K^{(\mathrm{OC})}} + \frac{b_K^{(\mathrm{OC})}}{a_K^{(\mathrm{OC})}}\right\}\right\}}{1+y}\,dy. \quad (51)$$

Let $z = \exp\left\{-\frac{y}{a_K^{(\mathrm{OC})}}\right\}$, we have $y = -a_K^{(\mathrm{OC})}\ln z$ and $dy = -\frac{a_K^{(\mathrm{OC})}}{z}\,dz$. Furthermore, for notational simplicity, we define $\eta = \exp\left\{\frac{b_K^{(\mathrm{OC})}}{a_K^{(\mathrm{OC})}}\right\}$. Thus, (51) can be rewritten as

$$R^{(\mathrm{OC})} \approx \frac{4}{\ln 2}\left[\int_{0^+}^{\frac{4}{\eta}} \frac{1-\exp\{-z\cdot\eta\}}{\left(1-a_K^{(\mathrm{OC})}\ln z\right)}\frac{a_K^{(\mathrm{OC})}}{z}\,dz + \int_{\frac{4}{\eta}}^1 \frac{a_K^{(\mathrm{OC})}\,dz}{\left(1-a_K^{(\mathrm{OC})}\ln z\right)z}\right]. \quad (52)$$

Recalling (49)-(50), we can easily see that the limit of the first term on the R.H.S. of (52) becomes vanishingly small as $\lim_{K\to\infty}\frac{4}{\eta} = 0$. Furthermore, the limit of the second term can be simplified as:

$$\lim_{K\to\infty}\frac{4}{\ln 2}\int_{\frac{4}{\eta}}^1 \frac{a_K^{(\mathrm{OC})}\,dz}{\left(1-a_K^{(\mathrm{OC})}\ln z\right)z} = \lim_{K\to\infty} 4\log\left(b_K^{(\mathrm{OC})}\right). \quad (53)$$

Thus, the corresponding scaling law is given by

$$\lim_{K\to\infty}\frac{R^{(\mathrm{OC})}}{4\log\left(b_K^{(\mathrm{OC})}\right)} = 1. \quad (54)$$

In particular, for $P_s = 1$, $b_K^{(\mathrm{OC})}$ and $a_K^{(\mathrm{OC})}$ can be approximated from (49)-(50) as:

$$b_{K,P_s=1}^{(\mathrm{OC})} \approx \ln 4K - 2\ln\ln K, \quad (55)$$

$$a_{K,P_s=1}^{(\mathrm{OC})} \approx 1, \quad (56)$$

and the resulting scaling law can be explicitly expressed as follows.

$$\lim_{K\to\infty}\frac{R_{P_s=1}^{(\mathrm{OC})}}{4\log\left(\ln 4K - 2\ln\ln K\right)} = 1, \quad (57)$$

which stands for a typical scaling law in the $\log\log K$ form.

C. Summary for schemes with MRC and SC

Following the same procedures, we can derive the average sum-rates and scaling laws for JOSRD with MRC and SC. More specifically, the CDFs of the parent effective SINR

obtained with MRC and SC for $M = 4$ and $N = 2$ are given by:

$$F_X^{(\mathrm{MRC})}(x) = 1 + \frac{x\exp\{-x/P_s\}\left(1-\frac{1}{P_s}\right)}{(1+x)^3} - \frac{\exp\{-x/P_s\}}{(1+x)^2} - \frac{3x\exp\{-x/P_s\}}{(1+x)^4}, \quad (58)$$

$$F_X^{(\mathrm{SC})}(x) = 1 - \frac{2\exp\{-x/P_s\}}{(1+x)^3} + \frac{\exp\{-2x/P_s\}}{(1+x)^6}. \quad (59)$$

Similarly, we can show that

$$R^{(\mathrm{MRC})} \approx \frac{4}{\ln 2}\int_0^\infty \frac{1-\exp\left\{-\exp\left\{-\frac{y}{a_K^{(\mathrm{MRC})}}+\frac{b_K^{(\mathrm{MRC})}}{a_K^{(\mathrm{MRC})}}\right\}\right\}}{1+y}\,dy, \quad (60)$$

and

$$R^{(\mathrm{SC})} \approx \frac{4}{\ln 2}\int_0^\infty \frac{1-\exp\left\{-\exp\left\{-\frac{y}{a_K^{(\mathrm{SC})}}+\frac{b_K^{(\mathrm{SC})}}{a_K^{(\mathrm{SC})}}\right\}\right\}}{1+y}\,dy. \quad (61)$$

The corresponding scaling laws take the following forms

$$\lim_{K\to\infty}\frac{R^{(\mathrm{MRC})}}{4\log\left(b_K^{(\mathrm{MRC})}\right)} = 1, \quad (62)$$

$$\lim_{K\to\infty}\frac{R^{(\mathrm{SC})}}{4\log\left(b_K^{(\mathrm{SC})}\right)} = 1. \quad (63)$$

In particular, for $P_s = 1$, the corresponding scaling laws can be shown as follows.

$$b_{K,P_s=1}^{(\mathrm{MRC})} \approx \ln 3K - 2\ln(1+\ln K), \quad (64)$$

$$b_{K,P_s=1}^{(\mathrm{SC})} \approx \ln 2K - 2\ln(1+\ln 2K), \quad (65)$$

$$a_{K,P_s=1}^{(\mathrm{MRC})} \approx a_{K,P_s=1}^{(\mathrm{SC})} \approx 1. \quad (66)$$

D. Comparison of results with numerical and approximated normalizing factors

Finally, we compare the average sum-rates shown in (51), (60) and (61) obtained with the numerical and approximated normalizing factors.

Figure 6 shows the average sum-rates derived with the numerical normalizing factors obtained by numerical methods for $P_s = 1$ and $P_s = 5$. Inspection of Fig. 6 reveals that (51), (60) and (61) agree well with the simulation results. Similar to the SIR-based analytical results, the SINR-based analysis is also very accurate for even smaller K values. Furthermore, Fig. 6 confirms that the scheduling scheme with OC can substantially outperform those with MRC and SC even in the presence of stronger noise. More specifically, for $P_s = 1$, JOSRD with OC outperforms those with MRC and SC by more than 10% and 20% in terms of throughput, respectively. The advantages of OC becomes more apparent as P_s increases.

Next, rather than the numerical solutions, Fig. 7 depicts the average sum-rates using the *approximated* normalizing factors computed in (55), (64) and (65) together with $a_{K,P_s=1} \approx 1$ for $P_s = 1$. Since the approximation expressions have been derived by assuming a large K, the analytical curves shown in Fig. 7 approach the simulated curves only when K becomes large. To inspect the approximation accuracy of (55), (64) and (65), Fig. 8 shows the numerical and approximated normalizing factors as a function of the number of MTs, K. Since solving the exact solutions to the normalizing factors involves the linear-exponential functions, it is in general non-trivial to obtain accurate closed-form expressions for the normalizing factors, which compromises the accuracy of the subsequently derived scaling laws.

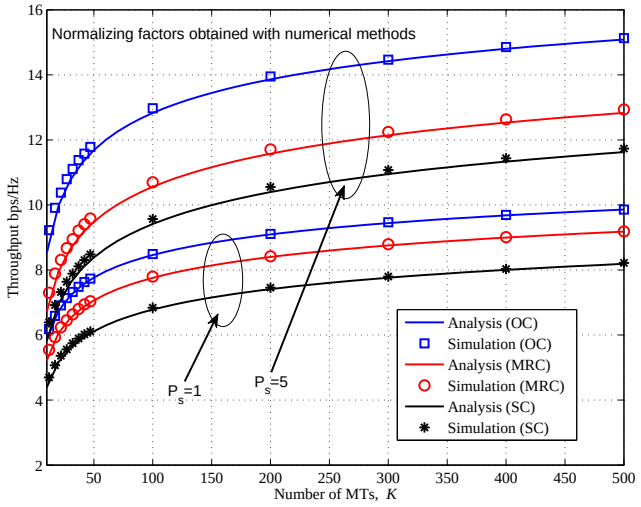

Fig. 6. Simulation versus analytical results with numerical normalizing factors for $P_s = 1, 5$.

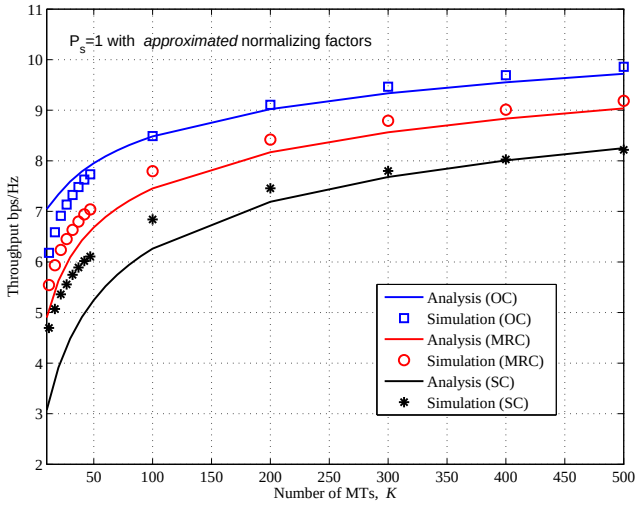

Fig. 7. Simulation versus analytical results with approximated normalizing factors for $P_s = 1$.

VI. Comparison between SIR and SINR-based analyses

The following remarks on the comparison of the SIR and SINR-based analyses are of interest.

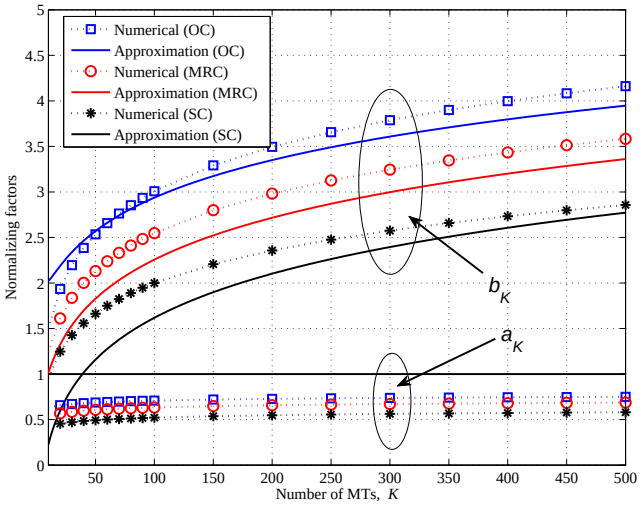

Fig. 8. Comparison of the numerical and approximated solutions of the normalizing factors for $P_s = 1$.

- On the one hand, it is easy to verify that the CDFs of the effective SINR shown in (41), (58) and (59) converge the corresponding CDFs of the effective SIR shown in (16), (15) and (14) with $M = 4$ and $N = 2$, respectively, as P_s tends to infinity. On the other hand, the SIR and SINR-based analyses suggest that the limiting distributions of the effective SIR and SINR do not belong to the same domain of attraction. Instead, they are of the Frechet-type and Gumbel-type, respectively. It is natural to conjecture that the limiting distribution function of SINR might also converge to the Frechet-type if P_s grows to infinity. However, our results reveal that this intuition is not true. This is because that the limit operator is *not* commutative in general, i.e. changing the order of two limit operators generally leads to different results.
- It is generally more difficult to obtain the normalizing factors in the SINR-based analysis than the SIR-based analysis since the SINR-based analysis involves exponential-type CDFs and requires solving exponential-linear equations such as (46). Therefore, it is more computationally advantageous to derive the scaling laws in the SIR-based analysis compared to the SINR-based analysis in the presence of strong interference.
- When computing the normalizing factors in the SINR-based analysis, we have to carefully take into account the high-order terms in $F_Y(y)$. For instance, if the high-order terms in $F_Y(y)$ in (58) and (41) are ignored, the resulting simplified CDFs for schemes with OC and MRC will all lead to the same set of normalizing factors, i.e. $\frac{\exp\{-b_K^{(\mathrm{OC})}/P_s\}}{\left(1+b_K^{(\mathrm{OC})}\right)^2} \approx \frac{\exp\{-b_K^{(\mathrm{MRC})}/P_s\}}{\left(1+b_K^{(\mathrm{MRC})}\right)^2} \approx \frac{1}{K}$. As a result, the performance of scheduling schemes with OC and MRC cannot be distinguished simply based on their scaling laws. Thus, caution must be exercised in evaluating the SINR-based scaling laws. On the other hand, since it is generally much easier to compute the normalizing factors with high accuracy in the SIR-based analysis, we argue that the SIR-based scaling laws can better characterize the actual performance of different scheduling schemes in the interference-limited scenarios.

VII. Simulation Results

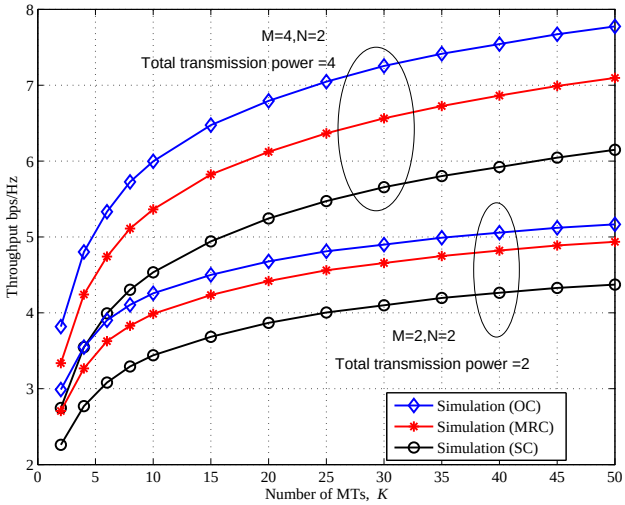

Fig. 9. Average sum-rates as a function of the number of MTs with total power equal to M for $M = 2, 4$, $N = 2$ and $P_s = 1$.

In this section, we use computer simulation to confirm the performance of JOSRD in different noisy scenarios. Figure 9 shows the average sum-rates of the JOSRD with $M = 2, 4$, $N = 2$ and $P_s = 1$. Fig. 9 indicates that the sum-rates of OC represents an impressive 20% and 10% increase compared to that of SC and MRC for $K = 50$, respectively. Note that the total transmission power for $M = 4$ is twice of that for $M = 2$ in Fig. 9. As a result, the average SNR for each beam is approximately constant.

In contrast, Figure 10 depicts the average sum-rates of JOSRD with $M = 2, 4$ and $N = 2$ for a *fixed* total transmission power of 2. It is evident from Fig. 10 that the sum-rate with $M = 4$ is higher than that with $M = 2$ for the same amount of total transmission power. This is because the effect of an increasing M on the average sum-rate is two-fold. On the one hand, a larger M creates more interference to a specific desired beam, which incurs loss of SINR. On the other hand, a larger M also linearly increases the system throughput as indicated in (12), which outweighs the throughput loss due to a reduced SINR as indicated in Fig. 10.

Throughout this work, our performance analysis was carried out by assuming the presence of a large number of MTs. In this last experiment, we examine the performance of different combining techniques with only a smaller number of MTs. Figure 11 shows the average sum-rates of a system with $M = 4$, $N = 2$ and $K = 5$ using different combining techniques.

Inspection of Figure 11 reveals that OC provides a substantially higher throughput gain as compared to SC and MRC. This is because the likelihood of having several users' channel vectors perfectly aligned to different orthogonal beams reduces

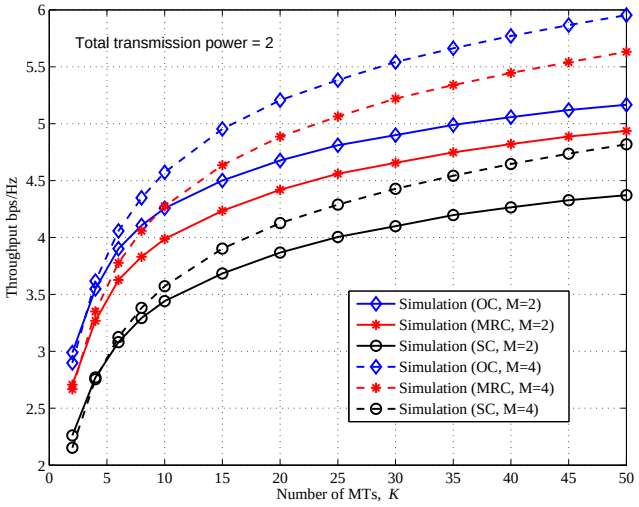

Fig. 10. Average sum-rates as a function of the number of MTs with total power equal to 2, $M = 2, 4$, $N = 2$ and $P_s = 1$.

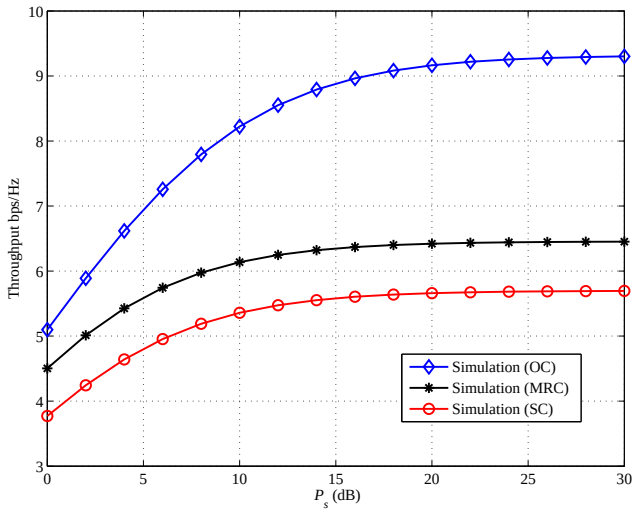

Fig. 11. Average sum-rates as a function of P_s with $K = 5$.

with the number of MTs. As a result, a receiver employing OC can provide more effective interference suppression, which leads to considerable performance improvement.

Finally, we examine the performance of reduced-feedback JOSRD (RF-JOSRD) discussed in Sec. III-C. Figure 12 compares the performance between JOSRD with $Q = M$ feedback and RF-JOSRD with $Q = 1$ (i.e. feeding back only the best beam information).

Inspection of Figure 12 suggests that the performance degradation due to reduced feedback is rather marginal for reasonably large networks (i.e. networks comprised of more than 15 MTs in our simulation). The same observation has been reported in [15], [17]. This can be partially explained by the fact that unitary codebooks are employed in this work. As a result, if a user has a channel closely aligned with one beamforming vector, then its channel is approximately orthogonal to other beamforming vectors. Since the effective

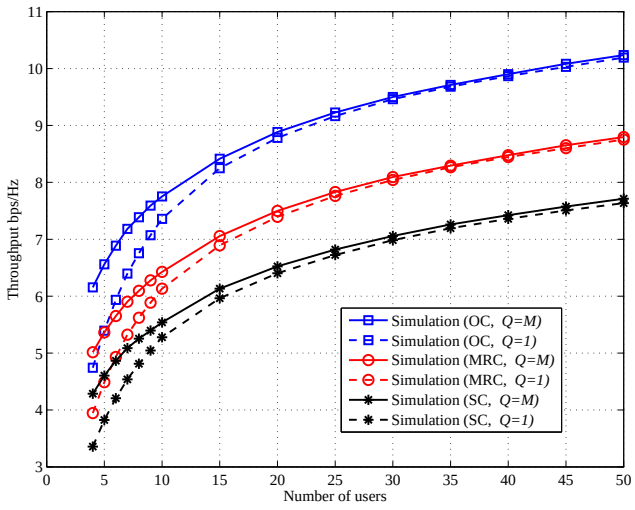

Fig. 12. Performance comparison between JOSRD and RF-JOSRD with $Q = 1$.

SINR associated with those orthogonal beams is rather small, feeding back the best beam information only incurs marginal performance degradation for large networks.

VIII. Conclusion and Future Work

Performance analysis on joint opportunistic scheduling and receiver design (JOSRD) for MIMO-SDMA downlink systems has been established in this work. Through asymptotic analysis and computer simulation, it has been shown that incorporating low-complexity yet effective linear combining techniques into the design of scheduling schemes for MIMO-SDMA downlink systems can substantially increase the system throughput. Furthermore, a systematic approach has been developed to derive the average sum-rates and scaling laws for OS schemes by utilizing extreme value theory [19]. In particular, our analytical results have shown that the limiting distribution of the effective SIR is of the Fretch type and the resulting scaling laws follow the $\epsilon \log K$ form for $0 < \epsilon < 1$ whereas the limiting distribution of the effective SINR is of the Gumbel type leading to the scaling laws governed by the conventional $\log \log K$ form. Simulation results have confirmed the effectiveness in improving system throughput by incorporating low-complexity linear combining techniques in OS schemes. Finally, it has been argued through comparison of SIR and SINR-based analyses that the SIR-based analysis is more computationally efficient for SDMA-based systems and it captures the asymptotic system performance with higher fidelity.

There are several extensions of this study that can be further explored. First of all, rather than setting M and N to some specific values in our sum-rate analysis, the feasibility of deriving a generalized expression for asymptotic sum-rate performance in terms of M and N remains an open question. Inspection of (38)-(40) may hint that such an attempt may be analytically intractable. However, such an expression will provide great insight into the impact of M and N on the system throughput. Furthermore, it will be of great practical interest to compare

JOSRD with other existing schemes proposed in the literature. However, caution has to be exercised in order to provide a fair view of these feedback schemes. A comprehensive comparison should take into account throughput performance, feedback overhead and computational complexity. In particular, further analysis to quantify the performance degradation of JOSRD and other existing schemes with respect to DPC is of great importance. Finally, throughout this work, homogeneous networks have been studied, which is commonly assumed in the literature. However, performance analysis on heterogeneous networks comprised of MTs with unequal SNRs stands for a more practical challenge that merits further investigation.

APPENDIX A: DERIVATION OF (27)

In this section, we provide the derivation details of (27).

$$\begin{aligned} & C^{(\mathrm{OC})} \\ = \; & -4\int_0^\infty \log(1+x)\, d\left[1-\exp\left\{-\frac{\left(\sqrt{3K}-1\right)^2}{x^2}\right\}\right], \\ = \; & -4\left\{\left[1-\exp\left\{-\frac{\left(\sqrt{3K}-1\right)^2}{x^2}\right\}\right]\log(1+x)\Big|_0^\infty \right. \\ & \left. -\int_0^\infty \left[1-\exp\left\{-\frac{\left(\sqrt{3K}-1\right)^2}{x^2}\right\}\right] d\log(1+x)\right\}, \\ = \; & \frac{4}{\ln 2}\int_0^\infty \frac{1-\exp\left\{-\frac{\left(\sqrt{3K}-1\right)^2}{x^2}\right\}}{1+x}\, dx. \end{aligned} \tag{67}$$

APPENDIX B: DERIVATION OF (49) AND (50)

Substitute (41) into (46), we have

$$\begin{aligned} & \frac{\exp\left\{-b_K^{(\mathrm{OC})}/P_s\right\}}{\left(1+b_K^{(\mathrm{OC})}\right)^2} + \frac{2b_K^{(\mathrm{OC})}\exp\left\{-b_K^{(\mathrm{OC})}/P_s\right\}}{\left(1+b_K^{(\mathrm{OC})}\right)^3} \\ & + \frac{b_K^{(\mathrm{OC})}\exp\left\{-b_K^{(\mathrm{OC})}/P_s\right\}}{P_s\left(1+b_K^{(\mathrm{OC})}\right)^3} = \frac{1}{K} \end{aligned} \tag{68}$$

Exploiting the following approximation for large $b_K^{(\mathrm{OC})}$

$$\frac{\exp\left\{-b_K^{(\mathrm{OC})}/P_s\right\}}{\left(1+b_K^{(\mathrm{OC})}\right)^2} \approx \frac{b_K^{(\mathrm{OC})}\exp\left\{-b_K^{(\mathrm{OC})}/P_s\right\}}{\left(1+b_K^{(\mathrm{OC})}\right)^3}, \tag{69}$$

we can rewrite (68) as

$$\frac{(3+1/P_s)\exp\left\{-b_K^{(\mathrm{OC})}/P_s\right\}}{\left(1+b_K^{(\mathrm{OC})}\right)^2} \approx \frac{1}{K}, \tag{70}$$

$$b_K^{(\mathrm{OC})} \approx P_s \ln\left((3+1/P_s)\,K\right) - 2P_s\ln\left(P_s\ln K\right). \tag{71}$$

Repeating the above computation on (47), we can show that

$$a_K^{(\mathrm{OC})} + b_K^{(\mathrm{OC})} \approx P_s\ln\left((3+1/P_s)\,Ke\right) - 2P_s\ln\left(P_s\ln K\right), \tag{72}$$

$$a_K^{(\mathrm{OC})} \approx P_s. \tag{73}$$

The result of $a_K^{(\mathrm{OC})} \approx P_s$ can be justified from the fact that the shape of the Gumbel-type limiting distribution is unaltered compared to the parent distribution. As a result, the random variable y in (45) is scaled by the same factor, i.e. P_s, as x in (41).

REFERENCES

[1] G. L. Stuber, J. R. Barry, S. W. McLaughlin, Y. Li, M. A. Ingram, and T. G. Pratt, "Broadband MIMO-OFDM wireless communications," *Proceedings of the IEEE*, vol. 92, no. 2, pp. 271–294, February 2004.

[2] G. Caire and S. Shamai, "On the achievable throughput of a multiantenna Gaussian broadcast channel," *IEEE Trans. Info. Theory*, vol. 49, no. 7, pp. 1691–1706, June 2003.

[3] P. Viswanath, D. N. C. Tse, and R. Laroia, "Opportunistic beamforming using dumb antennas," *IEEE Trans. Info. Theory*, vol. 48, no. 6, pp. 1277–1294, June 2002.

[4] I. Kim, S. Hong, S. S. Ghassemzadeh, and V. Tarokh, "Opportunistic beamforming based on multiple weighting vectors," *IEEE Trans. Wireless Commun.*, vol. 4, no. 6, pp. 2683–2687, November 2005.

[5] J. Chung, C. Hwang, K. Kim, and Y. K. Kim, "A random beamforming technique in MIMO systems exploiting multiuser diversity," *IEEE Journal Select. Areas Commun.*, vol. 21, no. 5, pp. 848–855, June 2003.

[6] M. Sharif and B. Hassibi, "On the capacity of MIMO broadcast channels with partial side information," *IEEE Trans. Info. Theory*, vol. 51, no. 2, pp. 506–522, February 2005.

[7] ——, "A comparison of time-sharing, DPC and beamforming for MIMO broadcast channels with many users," *IEEE Trans. Commun.*, vol. 55, no. 1, pp. 11–15, January 2007.

[8] W. Choi, A. Forenza, J. G. Andrews, and J. R. W. Heath, "Capacity of opportunistic space division multiple access with beam selection," in *Proc. IEEE Globecom 2006*, San Francisco, CA, November 2006.

[9] K. Huang, J. R. W. Heath, and J. G. Andrews, "Space division multiple access with a sum feedback rate constraint," *IEEE Trans. Signal Process.*, vol. 55, no. 7, pp. 3879–3891, July 2007.

[10] R. W. Heath, M. A. Jr., and A. J. Paulraj, "Multiuser diversity for mimo wireless systems with linear receivers," in *Proc. the IEEE Asilomar Conf. on Signals, Systems, and Computers*, Pacific Grove, California, November 2001, pp. 1194 –1199.

[11] M. Kobayashi and G. Caire, "Joint beamforming and scheduling for a multi-antenna downlink with imperfect transmitter channel knowledge," *IEEE Journal Select. Areas Commun.*, vol. 25, no. 7, pp. 1468–1477, September 2007.

[12] K. Huang, J. G. Andrews, and J. R. Heath, "Performance of orthogonal beamforming for sdma with limited feedback," *IEEE Transactions on Vehicular Technology*, vol. 58, no. 5, pp. 1959–1975, May 2009.

[13] N. Ravindran and N. Jindal, "Multi-user diversity vs. accurate channel feedback for mimo broadcast channels," in *Proc. IEEE International Conf. Commun. (ICC)*, Beijing, China, May 2008.

[14] T. Yoo, N. Jindal, and A. Goldsmith, "Multi-antenna downlink channels with limited feedback and user selection," *IEEE Journal Select. Areas Commun.*, vol. 25, no. 7, pp. 1478–1491, September 2007.

[15] N. Jindal, "Antenna combining for the mimo downlink channel," *IEEE Trans. Wireless Commun.*, vol. 7, no. 10, pp. 3834–3844, October 2008.

[16] M. Trivellato, F. Boccardi, and H. Huang, "Zero-forcing vs unitary beamforming in multiuser mimo systems with limited feedback," in *Proc. IEEE Inter. Symp. Personal, Indoor and Mobile Radio Commun. (PIMRC)*, Cannes, France, September 2008.

[17] ——, "On transceiver design and channel quantization for downlink multiuser mimo systems with limited feedback," *IEEE Journal Select. Areas Commun.*, vol. 6, no. 8, pp. 1494–1504, October 2008.

[18] R. A. Monzingo and T. W. Miller, *Introduction to Adaptive Arrays*. Wiley-Interscience, New York, 1980.

[19] E. J. Gumbel, *Statistics of Extremes*. Columbia University Press, New York, 1968.

[20] A. Shah and A. M. Haimovich, "Performance analysis of maximal ratio combining and comparison with optimal combining for mobile radio communications with cochannel interference," *IEEE Trans. Veh. Tech.*, vol. 49, no. 4, pp. 1454–1463, July 2000.

[21] H. Gao, P. J. Smith, and M. V. Clark, "Theoretical reliability of MMSE linear diversity combining in Rayleigh-fading additive interference channels," *IEEE Trans. Commun.*, vol. 46, no. 5, pp. 666–672, May 1998.

[22] B. D. Rao, M. Wengler, and B. Judson, "Performance analysis and comparison of MRC and optimal combing in antenna array systems," in *Proc. IEEE Int'l Conf. Acoust. Speech Signal Process*, Salt Lake City, UT, May 2001, pp. 2949–2952.

Man-On Pun (M'06) received the BEng. (Hon.) degree in electronic engineering from the Chinese University of Hong Kong in 1996, the MEng. degree in computer sciences from University of Tsukuba, Japan in 1999 and the Ph.D. degree in electrical engineering from University of Southern California, Los Angeles, in 2006, respectively. He is a research scientist at Mitsubishi Electric Research Laboratories (MERL), Cambridge, MA. He held research positions at Princeton University, Princeton, NJ from 2006 to 2008 and Sony Corporation in Tokyo, Japan, from 1999 to 2001. Dr. Pun's research interests are in the areas of statistical signal processing in wireless communications.

Dr. Pun received the best paper award - runner-up from the IEEE Conference on Computer Communications (Infocom), Rio de Janeiro, Brazil in 2009, the best paper awards from the IEEE International Conference on Communications, Beijing, China in 2008 and the IEEE Vehicular Technology Fall Conference, Montreal, Canada in 2006. He is a recipient of several scholarships including the Japanese Government (Monbusho) Scholarship, the Sir Edward Youde Memorial fellowship for Overseas Studies and the Croucher postdoctoral fellowship.

Visa Koivunen (SM'98) received the D.Sc. (Tech) degree (with honors) from the Department of Electrical Engineering, University of Oulu. From 1992 to 1995, he was a visiting researcher at the University of Pennsylvania, Philadelphia. From 1997 to 1999, he was an Associate Professor at the Signal Processing Laboratory, Tampere University of Technology. Since 1999, he has been a Professor of Signal Processing at Helsinki University of Technology (HUT), Finland. He is one of the Principal Investigators in SMARAD (Smart Radios and Wireless Systems) Center of Excellence in Radio and Communications Engineering nominated by the Academy of Finland. He has been also Adjunct Full Professor at the University of Pennsylvania, Philadelphia. During his sabbatical leave in 2006-2007, he was Visiting Fellow at Nokia Research Center as well as at Princeton University. Academy of Finland granted him the Academy Professor position in 2009.

His research interest include statistical, communications, and sensor array signal processing. He has published more than 300 papers in international scientific conferences and journals. Dr. Koivunen received the Primus Doctor (best graduate) Award among the doctoral graduates in years 1989 to 1994. He coauthored the papers receiving the Best Paper Award in IEEE PIMRC 2005, EUSIPCO 2006, and EuCAP 2006. He has been awarded the IEEE Signal Processing Society Best Paper Award for 2007 (coauthored with J. Eriksson). He served as an Associate Editor for IEEE Signal Processing Letters. He is a member of the Editorial Board for IEEE Transactions on Signal Processing, the Signal Processing journal and the Journal of Wireless Communication and Networking. He is also a member of the IEEE Signal Processing for Communication and Networking Technical Committee (SPCOM-TC) and Sensor Array and Multichannel Technical Committee (SAM-TC). He was the General Chair of the IEEE SPAWC (Signal Processing Advances in Wireless Communication) 2007 conference in Helsinki, Finland, in June 2007.

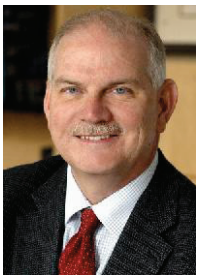

H. Vincent Poor (S'72, M'77, SM'82, F'87) received the Ph.D. degree in EECS from Princeton University in 1977. From 1977 until 1990, he was on the faculty of the University of Illinois at Urbana-Champaign. Since 1990 he has been on the faculty at Princeton, where he is the Michael Henry Strater University Professor, and Dean of the School of Engineering and Applied Science. Dr. Poor's research interests are in wireless networks and related fields. Among his publications in these areas are the books *MIMO Wireless Communications* (Cambridge University Press, 2007) and *Information Theoretic Security* (Now Publishers, 2009).

Dr. Poor is a member of the National Academy of Engineering, a Fellow of the American Academy of Arts and Sciences, and an International Fellow of the Royal Academy of Engineering of the U.K. He is also a Fellow of the Institute of Mathematical Statistics, the Optical Society of America, and other organizations. In 1990, he served as President of the IEEE Information Theory Society, and in 2004-07 he served as the Editor-in-Chief of the *IEEE Transactions on Information Theory*. He was the recipient of the 2005 IEEE Education Medal. Recent recognition of his work includes the 2009 Edwin Howard Armstrong Award of the IEEE Communications Society, the 2010 IET Ambrose Fleming Medal for Achievement in Communications, and the 2011 Eric E. Sumner Award.